0270-6474/85/0506-1641$02.00/0

The Journal of Neuroscience
Vol. 5, No. 6, pp. 1641-1652
June 1985

Selective Damage to Large Cells in the Cat Retinogeniculate Pathway by 2,5-Hexanedione[1]

TATIANA PASTERNAK,[2] DOROTHY G. FLOOD,* THOMAS A. ESKIN,‡ AND WILLIAM H. MERIGAN§

*Center for Brain Research and Center for Visual Science, University of Rochester, Rochester, New York 14627, and *Departments of Neurology and Anatomy, ‡Department of Pathology, and §Department of Ophthalmology, University of Rochester, School of Medicine and Dentistry, Rochester, New York 14642*

Abstract

The neurotoxic hexacarbon 2,5-hexanedione (2,5-HD), which produces transport abnormalities and swellings in the large diameter fibers of the peripheral nervous system, was administered to cats in an attempt to produce similar selective effects in the optic tract. Anatomical findings indicate damage to one type of retinal ganglion cell, the large (α) or Y-cell class, both during dosing and after a long recovery period. This selective involvement of the large ganglion cells during dosing was shown by decreased retrograde transport of HRP in these cells relative to smaller cells. Such selectivity was not apparent in axonal swellings and neurofilament accumulations which were present in fibers of all diameters in the distal optic tract. Visual threshold studies during dosing showed a loss of flicker resolution with preservation of visual acuity, a result consistent with the different physiological properties of α and β ganglion cells. In one cat, which survived dosing for a period of 8 months, there was a dramatic reduction in the number of large cells and a pronounced shrinkage of those that remained, but no observed changes in other cell types. Thus, this intoxication caused (*1*) axonal swellings which were not selective for fiber size; (*2*) a selective defect in axonal transport with later neuronal degeneration and shrinkage that were limited to large cells; and (*3*) a loss of flicker resolution that may reflect dysfunction of large ganglion cells.

The cat retina contains three morphological classes of ganglion cells that differ in soma size, axonal caliber, and dendritic morphology (Boycott and Wassle, 1974). α-Cells are rather sparse and have the largest somas, axonal diameters, and dendritic fields. β-Cells are more numerous and have smaller cell bodies, axonal diameters, and dendritic trees. Finally, γ-cells have even smaller somas and axonal diameters but large dendritic fields. Physiological counterparts of these three types of cells have been identified as Y-, X-, and W-cells, respectively (Cleland et al., 1975; Wassle et al., 1975). Neurophysiological studies of X- and Y-cells have revealed many differences in their receptive field properties, including differences in their response to high spatial and temporal frequencies (for review, see Lennie, 1980a). X-cells have smaller receptive fields and higher spatial resolution than Y-cells (Cleland et al., 1979; Linsenmeier et al., 1982). On the other hand, Y-cells are more sensitive to all temporal frequencies and have higher temporal resolution (Lennie, 1980b; Derrington and Lennie, 1983). While there is some agreement about the possible role of X-cells in visual function, the role of Y-cells is less well understood (see Lennie, 1980a). The study of their functional significance would be greatly facilitated if it were possible to damage or eliminate them without markedly affecting other classes of ganglion cells.

The present study is an attempt to produce such a selective effect in the cat retina. A similar approach was taken by Kornguth et al. (1982), who used antibodies to large ganglion cells and showed a reduction in the number of α-cells in the cat retina. We used the neurotoxic hexacarbon, 2,5-hexanedione (2,5-HD), which in the peripheral nervous system interferes with retrograde and anterograde transport (Sahenk and Mendell, 1981). This chemical causes neurofilament accumulation, axonal swellings in the distal portions of axons of the largest caliber and greatest length (Spencer and Schaumburg, 1975; Schaumburg and Spencer, 1979), and subsequent neuronal degeneration (Mendell and Sahenk, 1980). Similar swellings and neuronal degeneration are found in the central nervous system; among these, visual system changes are prominent (Schaumburg and Spencer, 1978; Griffiths et al., 1981; Jones and Cavanagh, 1982).

We examined changes in visual function, retrograde axonal transport, and morphology in the retinogeniculate pathway of cats intoxicated with 2,5-HD. Functional changes in vision were studied with behavioral measures of visual acuity and critical flicker frequency (CFF), which may be mediated by pathways of medium and large cells, respectively. We found that exposure to 2,5-HD produced deficits in CFF but not in visual acuity. This selective effect on one type of visual threshold was accompanied by reduced retrograde transport of HRP and subsequent degeneration of large (α) cells but not medium (β) cells.

Materials and Methods

Subjects and dosing procedures

Fourteen adult cats, both males and females, weighing between 2 and 5 kg were used. Five cats served as controls, and nine were dosed with 2,5-HD (Eastman Organic Chemicals). All but one dosed cat (cat 119) were maintained at 80 to 85% of their normal body weight. Water was continually available in their home cages, and they received a daily food supplement of Purina chow.

Received September 14, 1984; Revised November 30, 1984;
Accepted December 4, 1984

[1] This research was supported by Environmental Protection Agency Grant R8 09555 to W. H. M.; National Institute of Environmental Health Sciences Grant 01297 to T. P.; National Eye Institute Grants EY 05183 to D. G. F., EY 04118 to T. P., EY 01319 to the Center for Visual Science, and ES 10247 to the Environmental Health Sciences Center. Stephen Gilbert participated in early stages of this study, especially in the development of the jumping height test. We thank Laura Leinen, Deborah Gallant, Kiem van Nguyen, and Mary Kreutzer for excellent technical assistance. We also thank Mike King and Peter Lennie for the use of their laboratories and John McCrary for help with the statistical analysis.

[2] To whom correspondence should be addressed.

TABLE I

Dosages and experimental procedures for 2,5-HD-treated cats

Cats	Cumulative 2,5-HD Dose (ml/kg)	Days of Dosing	Behavioral Tests	Morphological Tests
8	7.3	56	Jump, Acuity, CFF	HRP (48),[a] LM[b]
88	4.7	52	Jump	LM
101	2.6	49	Jump, Acuity, CFF	HRP (48), LM, EM[c]
102	5.8	42	Jump, Acuity, CFF	HRP (48), LM, EM
109	5.8	48	Jump	LM, EM
119	4.7	38		LM
120	5.3	62	Jump	LM, EM, Nissl whole mount
122	5.8	50		HRP (24), LM, EM
126	5.6	38		HRP (24)
41	0.0	0		LM, EM
74	0.0	0		Nissl whole mount
107	0.0	0		HRP (24)
114	0.0	0		HRP (24)
125	0.0	0		HRP (48)

[a] Numbers in parentheses, hours of survival following HRP injection.

[b] LM, light microscopy of LGN and/or optic tract.

[c] EM, electron microscopy of LGN and/or optic tract.

Prior to the administration of 2,5-HD, the cats received their drinking water in a light-tight 240-ml bottle. During the administration of the neurotoxicant, the water was replaced by a 0.5% solution of 2,5-HD in distilled water. Fluid intake was monitored, and the solution was replaced daily. Dosing was discontinued after one or more of the following criteria were met: (*1*) the cats consumed more than 5 ml/kg total dose of 2,5-HD; (*2*) they showed hindlimb weakness as measured by a jumping test (see below); or (*3*) they were dosed for at least 38 consecutive days. Table I gives the doses of 2,5-HD for each cat, the dosing period, and the experimental procedures performed. All cats with the exception of cats 109 and 120 were sacrificed within two days of the termination of dosing. Cat 109 survived for 55 days and cat 120 for 8 months following exposure to 2,5-HD.

Behavioral testing

Before and throughout the dosing period, three of the experimental cats (8, 101, and 102) were tested daily on three behavioral tasks: visual acuity, flicker-fusion frequency, and maximal jumping height. The height test was used to assess hindlimb weakness, which is frequently observed in 2,5-HD intoxication (Jones and Cavanagh, 1982).

Visual acuity was measured by presenting stationary vertical sinusoidal gratings on one of two displays and a uniform field of the same mean luminance (17 cd/m^2) on a second. The stimuli were generated on Tektronix 606 oscilloscopes (P31-phosphor), subtended 11 × 14° visual angle at the 35-cm viewing distance, and had a surround of the same mean luminance as the displays extending out 22°. During each 200-trial session, the cats were tested in a chamber equipped with two adjacent optical glass response panels and a small feeding tube. The stimuli were viewed through the response panels, and a nose press response toward the display containing the grating was rewarded with pureed beef. A response towards the uniform field was followed by a 10-sec tone, and no reward was delivered. Trials were separated by a 5-sec intertrial interval. Initially, the cats were trained to discriminate a high-contrast (0.8; Michelson contrast was calculated as $I_{max} - I_{min}/I_{max} + I_{min}$, where I_{max} is luminance of the bright bar and I_{min} is the luminance of the dark bar of the grating), low-frequency (0.33 c/deg) grating from a uniform field. After the performance reached greater than 90% correct, threshold measurements began. Acuity was measured by varying the spatial frequency of gratings of 0.8 contrast. A staircase procedure, in which each correct response produced an increase in spatial frequency with probability of 0.3 and each incorrect response produced a decrease in spatial frequency, was used. The thresholds were taken from resulting psychometric functions at stimulus values corresponding to 75% correct responding.

Critical-flicker frequency was tested with the same display system and procedures as those for acuity measurements. The stimuli consisted of unpatterned fields, sinusoidally modulated in time, versus an unmodulated field of the same mean luminance (17 cd/m^2). The cats were rewarded for responding toward the flickering display. Initial training involved the discrimination between a 7-Hz flickering display and a spatially uniform, nonflickering field. Thresholds were measured with a procedure identical to that described above for acuity measurements.

The jumping test was designed to detect any diminution of hindlimb strength. Cats 8, 101, and 102 were trained to jump onto a 48 × 50 cm platform, which could be varied in height from 30 to 200 cm. Each successful jump was rewarded with food, and the height of the platform was raised 5 cm. Each session consisted of 5 to 6 jumps, starting with the height successfully negotiated in the previous session. Failure to jump was defined as either not hitting the platform despite an attempt, or no attempt to jump for 1 to 3 min. In that case, the platform was lowered by 5 cm. The jumping "threshold" was taken as the platform height reached at least twice during the session.

Each of the three cats were tested daily on the above tasks, with the jumping test usually following acuity and flicker measurements. The sequence of daily testing of the two visual functions was alternated. An additional three cats (cats 88, 109, 120) were tested on the jumping test only.

Retrograde axonal transport studies

On the day after dosing with 2,5-HD was discontinued, five of the cats (8, 101, 102, 122, and 126) were anesthetized with thiamylal sodium (Surital; 17.5 mg/kg of body weight i.v.) or with thiopental sodium (Pentothal; 20.0 mg/kg of body weight i.v.). Three undosed cats (107, 114, and 125) served as controls and were similarly anesthetized. The calvarium overlying the posterior thalamus was removed unilaterally (bilaterally for cat 107), and 4 or 5 injections were made along the length of the lateral geniculate nucleus (LGN). Each injection was 1 μl of 30% horseradish peroxidase (Sigma VI) dissolved in 2% dimethyl sulfoxide. In most cats, the injections were made stereotaxically. In cats 114, 122, and 126, the stereotaxic coordinates were corrected following isolation of single units in the LGN and mapping of the locations of their receptive fields. Cats survived 24 (cats 107, 114, 122, and 126) or 48 (cats 8, 101, 102, and 125) hr before receiving pentobarbital sodium (35 mg/kg of body weight i.v.) anesthesia. Intracardiac perfusion of 0.9% saline was followed by fixative consisting of 1% paraformaldehyde and 1.25 to 4% glutaraldehyde in 0.1 M phosphate buffer at pH 7.4.

The retinas were removed immediately and processed according to the tetramethyl benzidine (TMB) technique of Mesulam (1978). Retinas were rinsed in distilled water and preincubated in 5 mg of TMB and 100 mg of sodium nitroferricyanide in 2.5 ml of absolute ethyl alcohol, 92.5 ml of distilled water, and 5 ml of acetate buffer (0.2 M at pH 3.3) for 20 min at room temperature. Three ml of 0.3% hydrogen peroxide per 100 ml of preincubation solution were added while the retinas were gently agitated. The reaction was permitted to proceed until the incubation solution contained a blue precipitate—usually about 10 min. Retinas were then rinsed in acetate buffer solution (0.01 M), flattened, mounted on gelatinized slides, and allowed to dry overnight. The slides were then dehydrated quickly in 100% ethyl alcohol or acetone, cleared in xylene, and coverslipped with Permount. The TMB method produces some retinal shrinkage. We estimated the amount of this shrinkage by comparing the distance between the middle of the area centralis and the center of the optic disc to the value of 3.4 mm reported for normal adult by Hughes (1975). For the 11 retinas, the shrinkage ranged from 11 to 27% with a mean value of 18.2%. Since TMB is very labile in retinal preparations, the slides were kept frozen. This extended the life of the TMB

reaction product. Additionally, within 1 week of processing, the portions of the retinas containing labeled ganglion cells were completely photographed with EPY 135 Ektachrome film (Eastman-Kodak). The magnification of the 35-mm slides for the peripheral retina was × 25 and for the area centralis was × 50. The retinas were then traced with a Leitz projection system, and the locations of the 35-mm slides were identified on the drawings with the aid of blood vessels and cracks. A line was drawn through the optic disc and the area centralis on each retinal drawing. Lines 45° above and below this original line and extending from the area centralis were drawn in the region of labeled ganglion cells.

For counts of HRP-labeled ganglion cells, 35-mm slides along the two 45° lines were chosen at 2, 4, 6, 8, 10, and 12 mm eccentricity. These slides were projected. The original retinal preparations were used for counting ganglion cells at 0.5 mm eccentricity. At each eccentricity, an area of approximately 0.8 mm^2 was analyzed. The labeled cells were categorized into three groups according to size: (*1*) large ganglion cells corresponding to α-ganglion cells; (*2*) medium ganglion cells corresponding to β-ganglion cells and medium-sized γ-cells; and (*3*) small ganglion cells corresponding to γ-cells. We are using the term γ-cell broadly to include all of the various subtypes that have been described. Size criteria varied with eccentricity, but large ganglion cells were greater than 16 to 25 μm in diameter; medium ganglion cells were 11 to 25 μm; and small ganglion cells were less than 11 to 15 μm (Wassle et al., 1975; Stone, 1978; Hughes, 1981; Leventhal, 1982). Dendritic morphology was not used as a criterion for classification, since filling of dendrites was not always sufficient.

Density of HRP labeling was quantified for large ganglion cells and for medium ganglion cells. The 35-mm slides from the two 45° lines of each retina taken at 0.5, 2, 6, 10 and, in some cases, 12 mm eccentricity were projected onto a screen. A Tektronix J16 photometer was used to measure the luminances of each cell and the background next to the cell. In cases in which the background could not be used (e.g., pigment epithelium attached to the retina), the transmittances of adjacent large and medium cells were measured. These values were corrected for background luminances and were transformed into relative label by taking their reciprocals. Weakly labeled neurons, because of the greater sensitivity of the TMB technique than other methods (e.g., Mesulam and Rosene, 1979; Morrell et al., 1981), were also visible. The relative label of large to medium ganglion cells was assessed by calculating a ratio of label in each pair of large and medium ganglion cells. Pairs of cells used in this calculation were adjacent cells when no background density was measured; otherwise they were paired randomly. Because label was calculated in relative terms, problems of variations in HRP injection sites, TMB reactions, photography, etc. among cats were eliminated. Ratios of large cell HRP label to medium cell HRP label were then averaged, summing the two sampling lines and two retinas, for each eccentricity for each cat. Differences in ratios of HRP label for large and medium cell pairs among control cats and between dosed cats and the control group were evaluated with analysis of variance.

Examination of the optic tract and LGN

For processing of the HRP injection site, the block of tissue containing LGN was removed from the skull and placed in 10% sucrose in 0.1 M phosphate buffer at 4° C for several days. The block was then frozen and sectioned at 50 μm, and every fifth section was reacted with TMB as described above. Another set of adjacent sections was serially mounted on gelatinized slides and stained with cresyl violet. The boundaries of the LGN were drawn from the Nissl-stained sections, and the extent of the injection sites was determined with the corresponding TMB-reacted sections.

Thin (1 mm) blocks from the middle optic tract and LGN were osmicated and embedded in Poly 812 resin. Representative 1 to 2-μm sections were stained with toluidine blue for light microscopy. Thin sections were stained with uranyl acetate and lead citrate and examined on a Phillips EM 201.

Long-term survival study

One of the cats (cat 120) survived for 8 months following the end of dosing with 2,5-HD. It and a control (cat 74) were deeply anesthetized and perfused with 0.9% saline followed by 10% neutral buffered formalin. The right eyes were excised, and the retinas were dissected. Flattened retinas were mounted on gelatinized slides, stained with 1% cresyl violet, dehydrated, cleared, and coverslipped in Permount (Stone, 1981).

The retinas were traced at × 30 and eight lines 45° apart radiating from the area centralis were placed on each retinal drawing. Large ganglion cells were counted at × 300 along each of these lines at 2-mm intervals in a 0.388 to 1.55 mm^2 area and in area centralis in a 0.67 mm^2 area. Medium and small ganglion cells were counted in an area of 0.28 mm^2 along the two 45° lines (temporal and nasal fields) in the upper retinal field at 2 mm intervals at × 465 and were counted in an area of 0.01 mm^2 in the area centralis at × 1000. The criteria for cell classification were similar to those described above for HRP-labeled retinas. In addition, large cells could be identified by their polygonal shapes, caused by Nissl substance collecting at the bases of primary dendrites. Glia were usually about 5 μm in diameter, although some were greater than 7 μm. They were circular or elliptical in shape, with no apparent cytoplasm. Small ganglion cells differed from glia in size (usually greater than 7 μm) and cellular appearance. Their nuclei were pale relative to the cytoplasm and were surrounded by a more or less complete ring of Nissl substance. A nucleolus was often present, and the somas were often irregularly shaped. Displaced amacrine cells were not distinguished from ganglion cells in the ganglion cell layer. For all ganglion cell types, the counts from each line were combined at each eccentricity. Counts from eccentricities of 12, 14, and 16 mm (nasal hemifield only) were combined since they were similar and low. Differences between cats 120 and 74 in numbers of ganglion cells were statistically evaluated with the χ^2 test.

All large cells that were counted were also outlined on paper at × 300 for measurement. A total of sixty medium cells at each eccentricity were outlined in the locations in which they were counted. Medium cells in area centralis and at 2 to 4 mm eccentricity were drawn at × 750 and those from 6 to 16 mm eccentricity at × 465. The cell bodies were then traced on a graphics tablet and digitized by a microcomputer (Curcio and Sloan, manuscript in preparation). From the area of each cell body, the diameter was derived for a circle of equivalent area.

Results

Behavioral studies

Figure 1 shows visual acuity, critical flicker frequency, and jumping height for cats 8, 101, and 102 measured before and during dosing with 2,5-HD. The *data point* (± 1 SD) indicated at PRE is the mean threshold of 10 sessions immediately preceding the beginning of dosing. The other data points were collected during the dosing period; each is the mean of five thresholds collected in 1 week of testing.

Acuity of cat 8 decreased by approximately 8% at the beginning of the dosing period and remained at the slightly reduced level until the end of the experiment. It should be pointed out, however, that with the exception of weeks 3 and 4, the SDs of the control and dosing data overlapped and that, in the final week of dosing, acuity returned to the predosing range. Visual acuity of the other two cats (101 and 102) remained unchanged throughout the dosing period.

The second column of Figure 1 shows flicker resolution (CFF). In all three cats, CFF dropped in the second or third week of dosing by approximately 13 to 19% and remained reduced throughout the dosing period. It is important to note that, once decreased, the thresholds showed no indication of further change. The largest CFF loss was found in cat 102, in which the thresholds decreased from 55.6 to 43.6 Hz (21.6% loss).

Finally, the jumping data (third column of Figure 1) show that motor deficits appeared in the fourth or fifth week of dosing, some 2 to 3 weeks after the flicker deficits became apparent. Also note that, unlike CFF, jumping deficits became progressively more severe and, in the last testing session, the loss ranged from 30 to 50%. Jumping deficits of cats 88, 109, and 120 (not shown here) appeared within 4 to 6 weeks from the beginning of dosing and were similar to those shown in Figure 1.

Retrograde axonal transport studies

Injection sites. All injections could be categorized into one of two types. The first type included only the anterior LGN, resulting in labeling of contralateral nasal and ipsilateral temporal fields of the upper retina (cats 8, 102, 107, and 125). The second type included the entire LGN and the optic tract, resulting in labeling of the entire contralateral nasal and ipsilateral temporal retinal hemifields (cats 101, 114, 122, and 126). Labeling of small ganglion cells in the entire contralateral temporal field which project to the superior colliculus (Wassle and Illing, 1980) was found in cases of suspected optic tract injections. Additionally, rarely labeled cells (mostly medium in size) in the ipsilateral nasal field, described by Leventhal (1982),

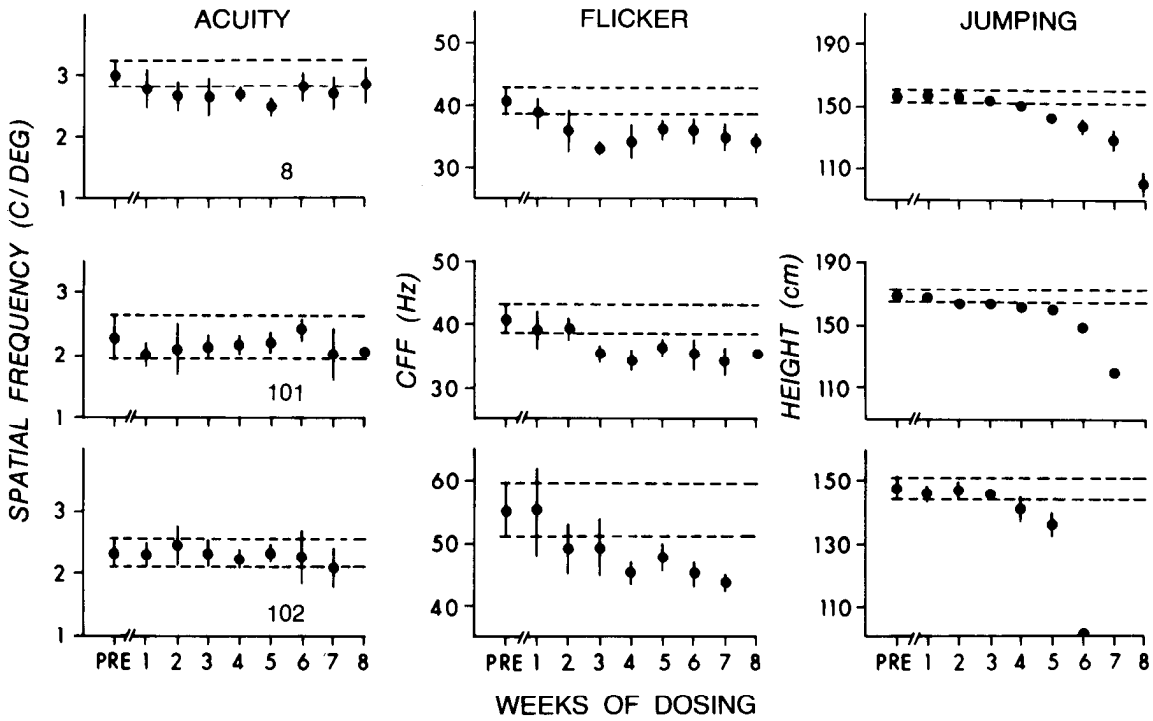

Figure 1. Visual acuity, critical flicker frequency (CFF), and jumping height for three cats measured before and during the administration of 2,5-HD. The *data point* (± 1 SD) indicated as PRE is a mean threshold of ten sessions immediately preceding the beginning of dosing. The other *data points* were collected during the dosing period, and each is a mean of five thresholds obtained in 1 week of testing. The points at which no *SD bars* are shown indicate either only one day of data collection (cat 101; the *last points* in acuity and flicker plots) or a SD smaller than the size of the symbol). The *dotted lines* across each graph indicate ± 1 SD of base line performance.

were found in cats 101, 114, 122, and 126. Both of these findings confirm inclusion of the tract in the injection sites for these cats. All cats had labeling of large cells and medium-sized γ-cells within 10 to 15° of the vertical meridian in the contralateral temporal field. Although these cells can be labeled from injections of the optic tract (since they project to the superior colliculus), a similar pattern of labeling can result from injections of layer 3 of the medial interlaminar nucleus (MIN) (Rowe and Dreher, 1982). The cats with more restricted injection sites (8, 102, and 125) included labeling of ganglion cells consistent with an MIN injection. Thus, it is likely that MIN was included in the injection sites of all cats.

In the contralateral nasal and ipsilateral temporal retinal hemifields, all cats showed labeling of medium-sized γ-cells. This pattern of labeling suggests that the injections may have included one or more of the following regions: C laminae of the LGN, ventral lateral geniculate nucleus, layers 1 and 2 of MIN and the retinal recipient zone (RRZ) of the pulvinar (Leventhal et al., 1980; Leventhal, 1982; Rowe and Dreher, 1982). A few small ganglion cells were labeled in the contralateral nasal and ipsilateral temporal hemifields in the cat with more restricted injections (e.g., cat 8), while in cats with optic tract injections, a large number of these cells was labeled. The presence of these cells indicates that C laminae of the LGN and ventral lateral geniculate nucleus were included in the injection sites (Leventhal, 1982; Rowe and Dreher, 1982). HRP was found in all of these areas, but we are uncertain as to how much of the injection site constitutes the area where axons or terminals were actively taking up HRP for transport to the retina.

Numbers of labeled ganglion cells. Figure 2 shows the counts of HRP-filled large and medium ganglion cells in control and dosed animals. The cell densities are shown separately for contralateral and ipsilateral retinal hemifields. Each *data point* is a group mean. There are more medium cells than large cells in both dosed and control cats, and there are no systematic differences between the dosed and control cats in numbers of medium and large ganglion cells. Both groups show lower numbers of labeled cells in the ipsilateral than in the contralateral hemifield. The total number of retrogradely labeled large and medium cells and the difference between the ipsilateral and contralateral hemifields are consistent with the recent report by Leventhal (1982), despite the fact that our injections were much larger and not limited to A laminae of the LGN. The agreement between Leventhal's and our estimates of the β-cell population is not surprising, since the numbers of medium-sized γ-cells projecting to the LGN are relatively modest (20%) as compared to the numbers of β-cells (Leventhal, 1982), and their inclusion would not substantially alter the overall number of medium-sized cells.

Small ganglion cells were variably filled, depending upon the depth of the HRP injection site. High injections filled few small ganglion cells; injection sites that included the C laminae of the LGN filled more small cells; and finally, injections of the optic tract filled the largest number of small cells. Since injections of the LGN alone do not optimally and reliably produce retrograde labeling of small ganglion cells, we have not quantified filling of this cell group.

Analysis of HRP label in ganglion cells. Differences in the density of HRP label between normal and 2,5-HD-dosed cats were apparent upon visual inspection of the retinas. In control cats (107, 114, and 125), large and medium ganglion cells appeared approximately equal in HRP density (Fig. 3*A*). Figure 3*B* shows the appearance of labeled retinas in one of the dosed cats (cat 102). Here, a difference in the density of HRP labeling in large and medium cells can be seen. While medium ganglion cells were heavily filled with purple-black granules of HRP, large ganglion cells had many fewer granules and appeared diffusely labeled. In the original material, in addition to differences in the density of HRP granules, one finds differences in color, with the large cells often having a pale blue-green appearance.

In other 2,5-HD dosed cats (8, 122, and 126), large ganglion cells were also found to be lighter than medium cells. Cat 101, which received less than half the dose given to other cats, was an exception. In this cat, the difference in label in large and medium ganglion cells was less apparent throughout the central portion of both retinas. However, large cells appeared much lighter in regions

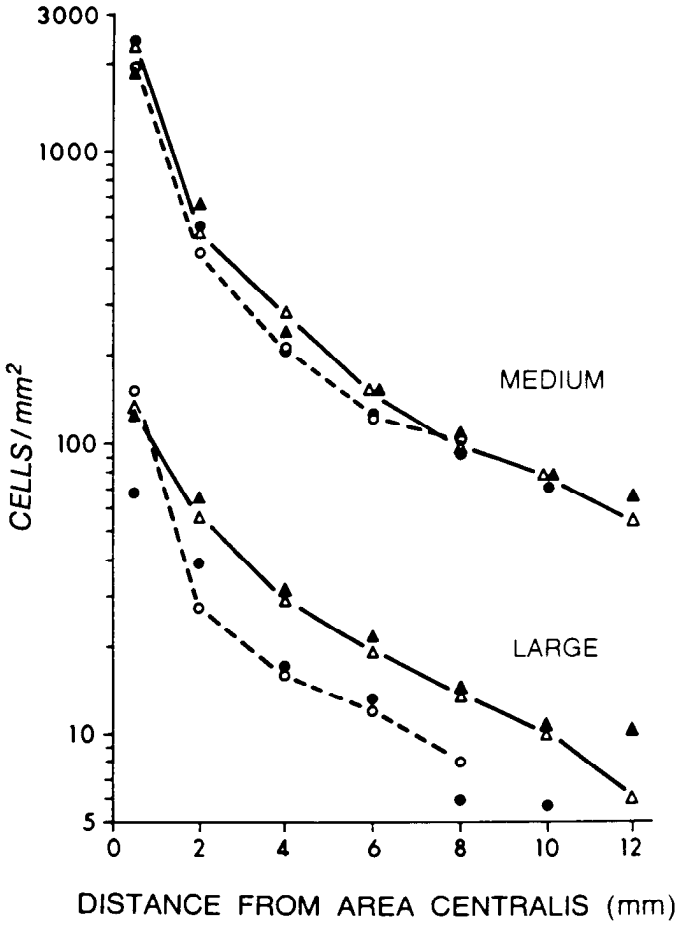

Figure 2. Mean densities of medium and large HRP-filled ganglion cells as a function of eccentricity in control (*open symbols*) and dosed (*solid symbols*) cats. Nasal (*triangles*) and temporal (*circles*) hemifields are plotted separately. The data for the control cats are connected by *solid lines*, while those for the dosed cats are *unconnected.*

of the retina covered by pigment epithelium, the far periphery. HRP labeling of small ganglion cells was quite variable in both normal and dosed cats, and no systematic differences between the two groups were apparent This variation could be primarily attributed to differences in the availability of HRP for uptake at the injection sites.

The differences in label density between the large and the medium cells found in the dosed cats were quantified by photometry. In Figure 4, mean ratios of label in large to medium cells are plotted as a function of the distance from area centralis. The data for the three normal cats (*open symbols*), which were not significantly different from each other ($p > 0.05$), are averaged and replotted in each graph for comparison. Individual data for the five dosed cats are plotted separately. A ratio of 1.0 indicates no difference in labeling between the two cell types. A ratio of 0.5 indicates that the label in large cells is two times weaker (i.e., the cell is lighter) than the label in medium cells. An overall analysis of variance revealed significant effects of 2,5-HD on labeling of large cells in cats 8, 102, 122, and 126 ($p < 0.001$) and 101 ($p < 0.003$). In all cats, both normal and dosed, the ratio of label in large to medium cells declined significantly with eccentricity. However, the effect of 2,5-HD on HRP transport in large cells did not vary with eccentricity. Subsequent tests for simple effects compared the relative ratios at each eccentricity in dosed and control animals. The ratios were significantly lower ($0.01 > p > 0.0001$) in dosed relative to normal cats in all cases, with the exception of cat 122 in the area centralis ($p > 0.05$). Cat 101, that which received the lowest dose of 2,5-HD, was an exception. Although at each eccentricity the label in large cells was somewhat less intense than in medium cells, these differences were not significant.

Optic tract and LGN

Several dosed animals (cats 8, 88, 102, 109, 119, and 122) had marked swellings of axons in the distal optic tract and LGN at the light microscopic level (Fig. 5*A*), when compared to normal (Fig. 5*B*). The swellings were present in axons of all diameters, and they were clearly visible by light microscopy in all cats except the cat that received the lowest dose of 2,5-HD (cat 101).

Electron microscopy revealed swollen large and medium diameter axons in the LGNs of all cats, including cat 101, that were filled with dense accumulations of 10-nm filaments and surrounded by disproportionately thin myelin sheaths (Fig. 6). In cat 109, that which survived for 55 days after the termination of dosing, degenerating axons and myelin profiles were also observed.

Long-term survival study

Figure 7 shows photomicrographs of the retinas of the cat that survived for 8 months after dosing (cat 120) and a control (cat 74) taken at 2 mm eccentricity. Here and elsewhere in the retina of cat 120 (Fig. 7*B*), the large ganglion cells were reduced in number and in size, compared with the control (Fig. 7*A*). No qualitative changes were apparent in numbers of smaller ganglion cells or glia. At greater eccentricities (the far periphery), medium ganglion cells appeared shrunken.

Numbers of large, medium, and small ganglion cells as a function of distance from area centralis are illustrated in Figure 8*A*. Large ganglion cells were significantly reduced in numbers by 36 to 69% (average = 49%) at eccentricities of 2 to 16 mm in cat 120 ($\chi^2 = 30.33$; df = 5; $p < 0.001$). The greatest reduction in large ganglion cells was found at 2 mm eccentricity. In area centralis, no loss of large ganglion cells was found. Medium and small ganglion cells were unchanged in numbers at all eccentricities in cat 120 (medium cells: $\chi^2 = 4.48$; df = 6; $p > 0.7$; small cells: $\chi^2 = 2.87$; df = 6; $p > 0.8$).

Medium-sized cells in cat 120 were unchanged in the measure of cell body diameter except at 2 and 12 to 16 mm eccentricities (Fig. 8*B*). At 2 mm, they were 5% larger in cat 120 than in the control cat; and at 12 to 16 mm eccentricities were 6% smaller in cat 120 than in the control. There was a slight reduction in medium cell size at 12 to 16 mm as compared with 4–10 mm eccentricity in the control cat. The measures at 12 to 16 mm represent only the contralateral retina, and that hemifield contains slightly smaller cell sizes (Leventhal, 1982). At all eccentricities, large ganglion cells in cat 120 were reduced in size by 4 to 15% compared with cat 74. Figure 8, *C* and *D*, illustrates frequency histograms for the diameters of large and medium cells from area centralis and eccentricities of 2 to 16 mm. The histograms of large cells (Fig. 8*C*) for area centralis are similar for both cats but show a slight size reduction for cat 120. At eccentricities of 2 to 16 mm, the histogram for cat 120 has been shifted to the left by approximately 4 to 5 μm, as compared with the data for the normal cat. This shift indicates a 4 to 5 μm shrinkage of the remaining large cell bodies in the dosed cat. In contrast to the large cells, the histograms for the medium cells (Fig. 8*D*) are nearly identical for the normal and the dosed cat, indicating that the size of these neurons remained unchanged.

Examination of the optic tract and LGN of cat 120 by light and electron microscopy revealed profound abnormalities. In the light microscope, the ventral portion of the optic tract appeared to have a reduced number of the very largest fibers (Fig. 5*C*). Other fibers appeared comparable in number to those in control animals. Electron microscopic examination of the ventral portion of the tract revealed evidence of an increased number of astroglial processes and an increased separation between myelinated fibers compared to controls.

Cells in the medial interlaminar nucleus (MIN) of the dosed and the control cat were examined under light microscopy. In the dosed

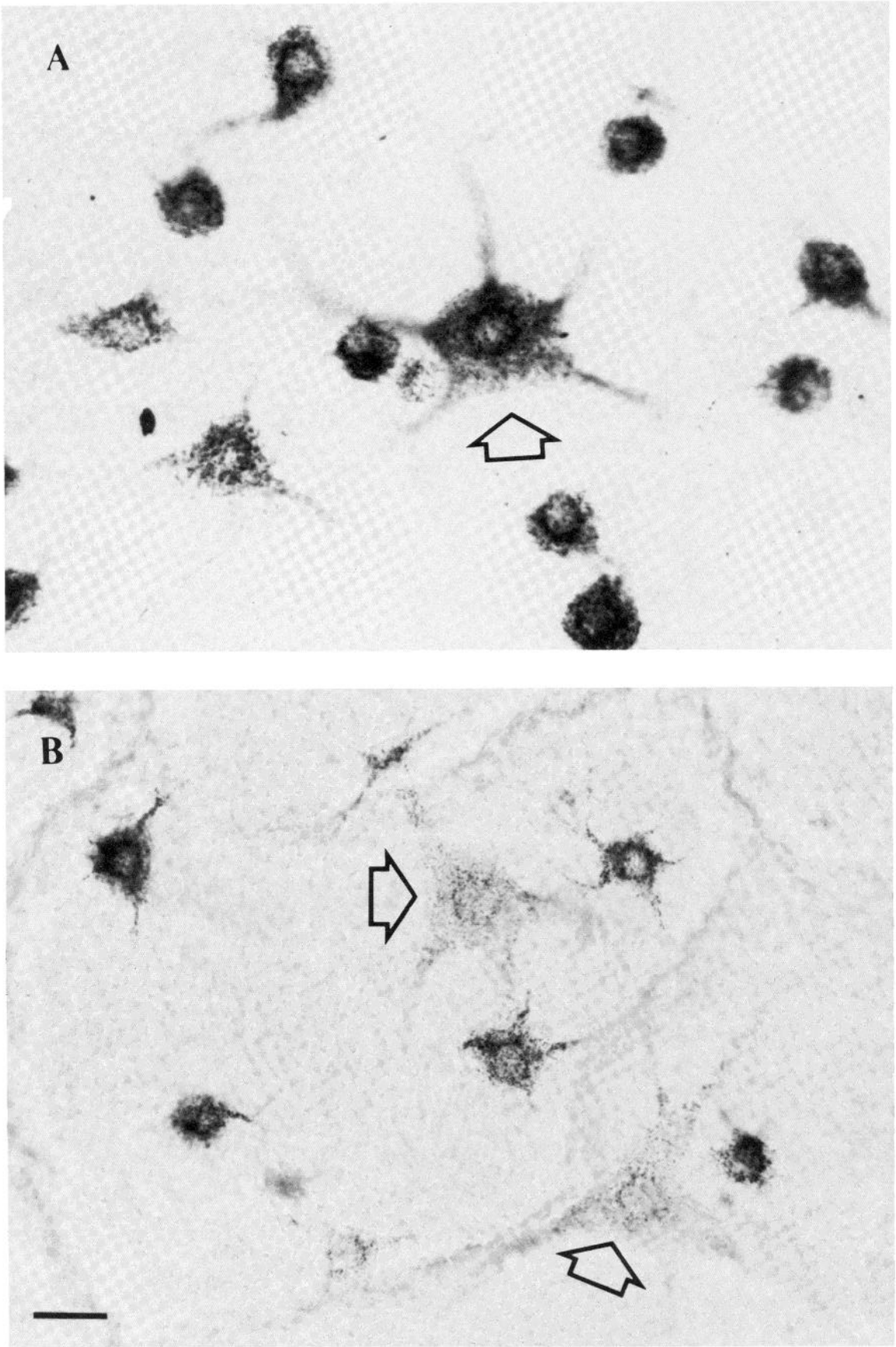

Figure 3. Photomicrographs of HRP-filled cells in normal (*A*) and 2,5-HD-dosed (*B*) cats. Note a well-labeled large cell (indicated by an *arrow*) in the control (cat 125) and two weakly labeled large cells (indicated by the *arrows*) in the dosed (cat 102) retina. In both retinas, the medium cells were well-filled *Scale bar* equals 20 μm.

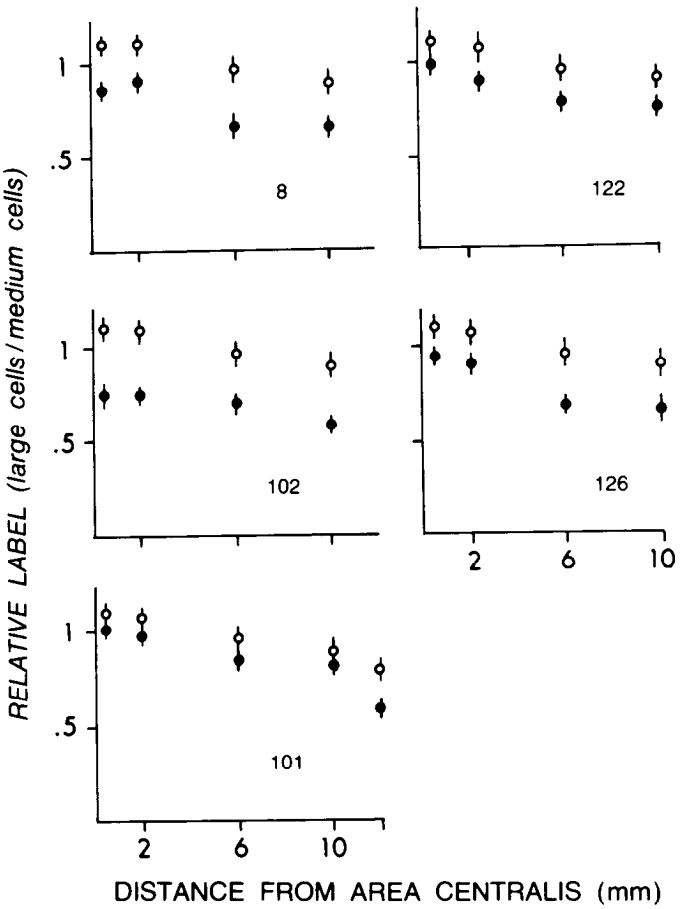

Figure 4. Relative HRP label as a function of eccentricity for the five dosed cats. Relative label was the ratio of the intensity of HRP label in large and medium cells as determined by photometry (see "Materials and Methods"). Each *data point* is a mean of at least 20 ratios, and the *bars* are ± 1 SEM. The data for the three control cats (*open circles*) were averaged, since they were not significantly different from each other. The control data are replotted in each of the five graphs to facilitate comparison with the 2,5-HD data (*solid circles*).

cat, the largest cells appeared somewhat smaller than those in the control, and there was subtle evidence of gliosis.

Discussion

Main findings. Anatomical findings indicate a selective damage to one type of retinal ganglion cell, the α- or Y-cell class, both during dosing and after a long recovery period. Visual threshold studies showed a loss of flicker resolution with preservation of visual acuity, a result consistent with the different physiological properties of the damaged (large) and undamaged (medium) ganglion cells. Selective involvement of the large ganglion cells was seen at the termination of the dosing period as a decreased retrograde transport of HRP in these cells relative to smaller cells. Flicker resolution dropped early in dosing and remained subnormal, while acuity was stable up to the time of the transport studies. In one cat, which survived dosing for a period of 8 months, there was a dramatic reduction in the number of remaining large cells and a pronounced shrinkage of those that remained, but no observed changes in other cell types.

Psychophysical results. Visual tests for the present study were chosen on the basis of differences in the sensitivity to high spatial and temporal frequencies of the large-sized Y-cells and medium-sized X-cells. While X-cells in the retina and LGN respond to higher spatial frequencies (Cleland et al., 1979; Derrington and Fuchs, 1979; Lehmkuhle et al., 1980; So and Shapely, 1981; Linsenmeier et al., 1982; Troy, 1983), Y-cells are more sensitive to all temporal frequencies and have higher temporal resolution (Lehmkuhle et al., 1980; Lennie, 1980; Troy, 1983). A selective effect on CFF, in the absence of acuity deficits, would suggest that the neurons with better temporal resolution (i.e., Y-cells) may be affected by 2,5-HD.

Flicker resolution in humans increases with eccentricity when large targets are viewed (Hylkema, 1942; Hartmann et al., 1979). Although comparable behavioral data for the cat are not available, single unit recordings from cat LGN show that peripheral Y-cells have higher temporal resolution than central Y-cells (Lehmkuhle et al., 1980). Thus, loss of the flicker resolution observed in the dosed cats may be indicative of damage to more peripherally located Y-cells. This loss of temporal resolution does not necessarily indicate dysfunction of Y-cells located in the central retina.

The relatively intact visual acuity of the cats throughout 2,5-HD intoxication suggests that any involvement of centrally located X-cells is unlikely. However, effects on more peripheral X-cells cannot be ruled out, since these neurons are probably not involved in visual acuity in cats with intact area centralis (Blake and di Gianfilippo, 1980; Pasternak et al., 1983).

The 15 to 20% loss in CFF was consistent with the small reported difference in temporal resolution between X- and Y-cells (e.g., Troy, 1983). Thus, the change in CFF may reflect conduction block in Y-cells with the transmission of high temporal frequency information depending on the less sensitive X-cells. It is also possible that the affected Y-cells were still functional but that their temporal resolution was reduced. Preliminary results of single unit recordings from the LGN of these cats show a reduction in the proportion of the encountered Y-cells, as well as a loss in sensitivity to all temporal frequencies in the remaining Y-cells, in the absence of detectable changes in X-cells (Scammel, manuscript in preparation). This result is entirely consistent with our behavioral data.

Retrograde transport. The selective reduction in transport in α-cells might be due to any of the differences between α-cells and smaller ganglion cells. The most prominent differences are in soma size and the cross-sectional area of axons. However, ganglion cell classes also differ in the size and structure of their dendritic fields (Boycott and Wassle, 1974), locus of central projections, extent of axonal branching (Illing and Wassle, 1981), and possibly in neurotransmitters (Ikeda and Sheardown, 1982). One finding in the present study suggests that it was in fact soma size and the greater axonal caliber that caused the greater transport reduction in α-cells. While a dramatic reduction in transport was found in the α-cells of most cats throughout the retina, this effect was seen only outside of the area centralis in two of the animals. Cat 122 showed significant transport defects only at eccentricities beyond the area centralis, while in the cat that received the lowest dose of 2,5-HD (cat 101), the deficits were dramatic only in the α-cells with the longest axons, those located 12 to 16 mm outside of area centralis. Our data and that of others (Boycott and Wassle, 1974; Wassle et al., 1975; Peichl and Wassle, 1979; Leventhal, 1982) show that the soma sizes of both α- and β-ganglion cells are considerably smaller in the area centralis than at eccentricities beyond 2 to 4 mm and that there is only a slight overlap in size between peripheral β-cells and central α-cells. Thus, it is likely that the greater soma and axon sizes and possibly axonal length of the eccentric α-cells were responsible for their susceptibility to the effects of 2,5-HD. In cats that showed a transport defect in α-cells throughout the retina, the minimal size consistent with a transport defect may have been just greater than the largest peripheral β-cells. Dendritic field size did not appear to contribute to the vulnerability of α-cells, since γ-cells, like α-cells, have large dendritic fields but did not show reduced transport.

A more pronounced effect on large fibers is in fact characteristic of 2,5-HD in the peripheral nervous system (Schaumburg and Spencer, 1979), and the basis of this selectivity is suggested by the nature of 2,5-HD's axonal changes. 2,5-HD causes disorganization of the axonal cytoskeleton (Griffin et al., 1983) with accumulation of neurofilaments and eventual development of neurofilamentous axonal swellings (Cavanagh and Bennetts, 1981). The rates of both

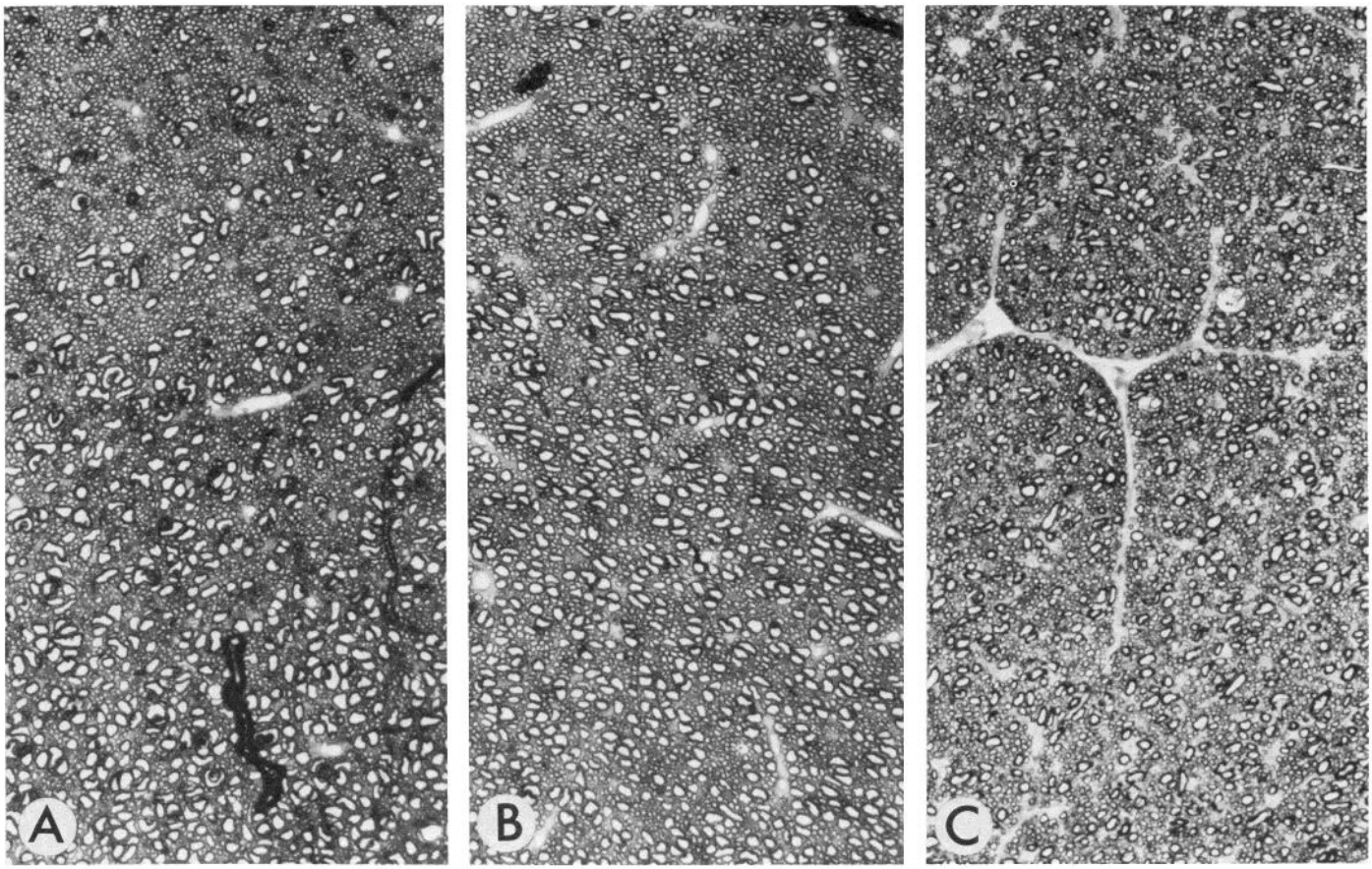

Figure 5. Photomicrographs of cross-sections through midoptic tract of two dosed (*A* and *C*) and one control (*B*) cats. Axons appear as rounded-to-irregular open profiles outlined by dark ring-shaped myelin sheaths. The ventral tract (*lower part* of each figure) contains a greater proportion of large-diameter fibers than the dorsal tract (*upper part* of each figure). *A*, Slightly swollen axons (compare the largest profiles with those shown in *B*) in cat 102 that was sacrificed immediately after dosing. *B*, Normal axons in an undosed control (cat 41). *C*, Reduced numbers of large fibers in the ventral tract of a cat that survived dosing for 8 months (cat 120). Toluidine blue. Magnification × 200.

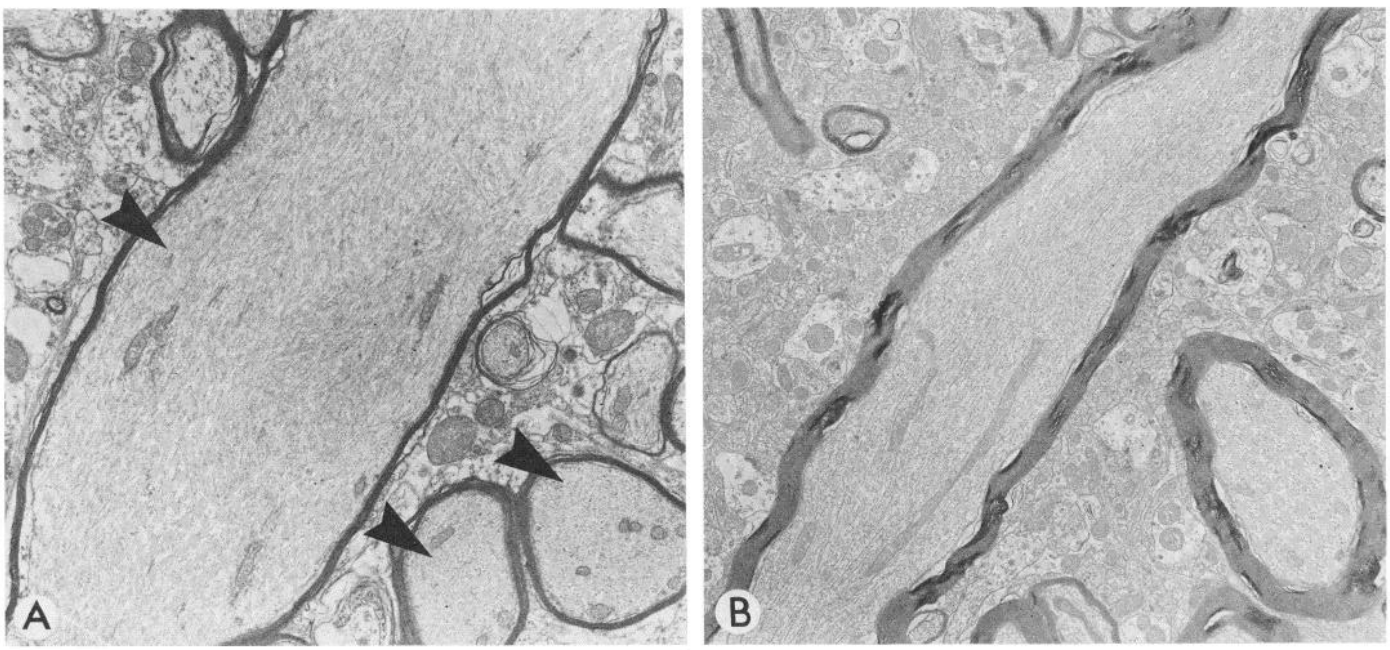

Figure 6. A, Electron micrograph of filamentous axonal swellings (indicated by *arrowheads*) in the LGN of a dosed cat (cat 122). *B*, Axons in a comparable region from a control (cat 41). Magnification × 6000.

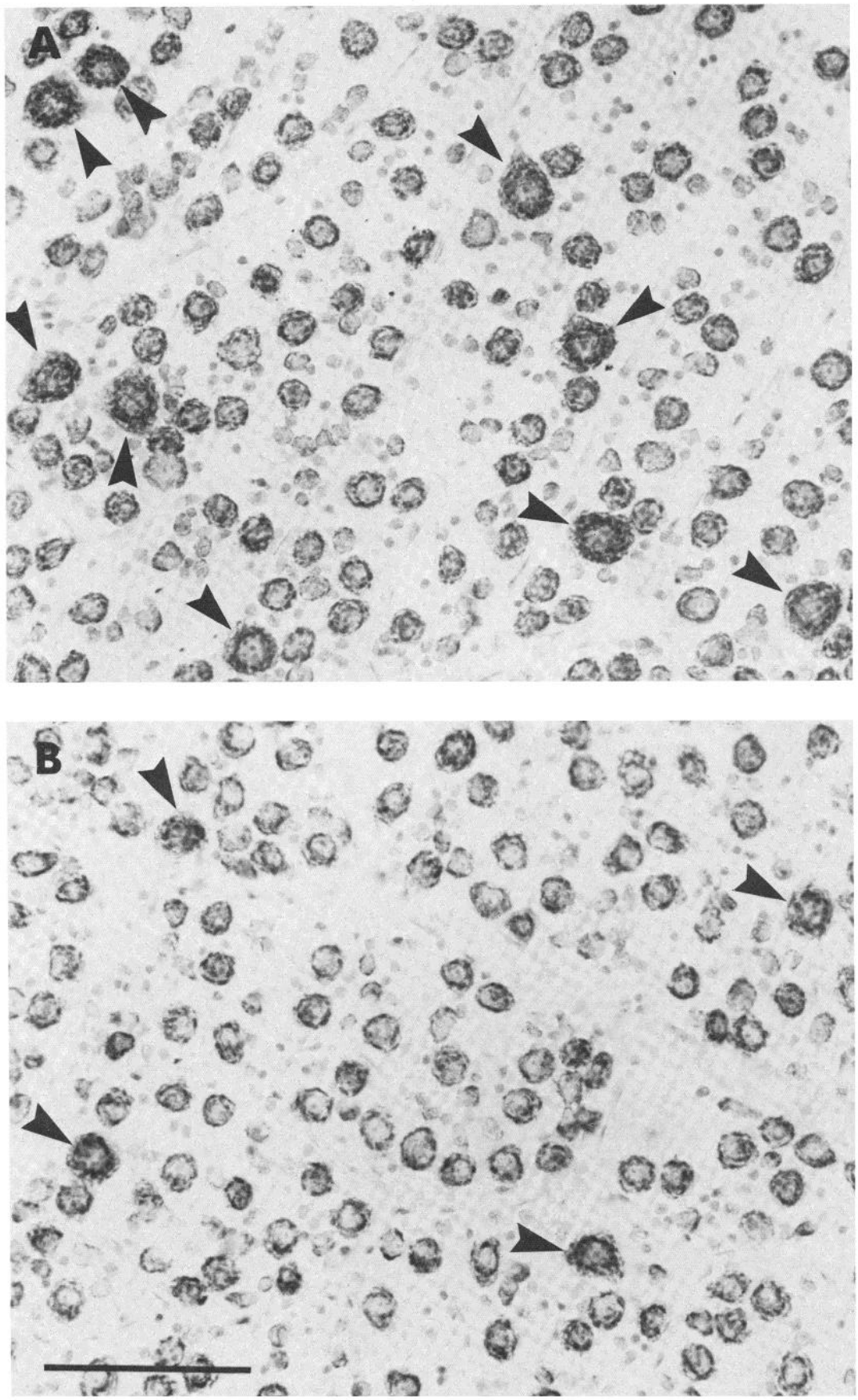

Figure 7. Photomicrographs of Nissl-stained retinal whole mounts from a control (cat 74) (*A*) and from a 2,5-HD-dosed animal (cat 120) that survived for 8 months (*B*) at 2 mm eccentricity. *Arrowheads* point to large ganglion cells, which are fewer in number and smaller in size in cat 120 than in cat 74. *Scale bar* equals 100 μm.

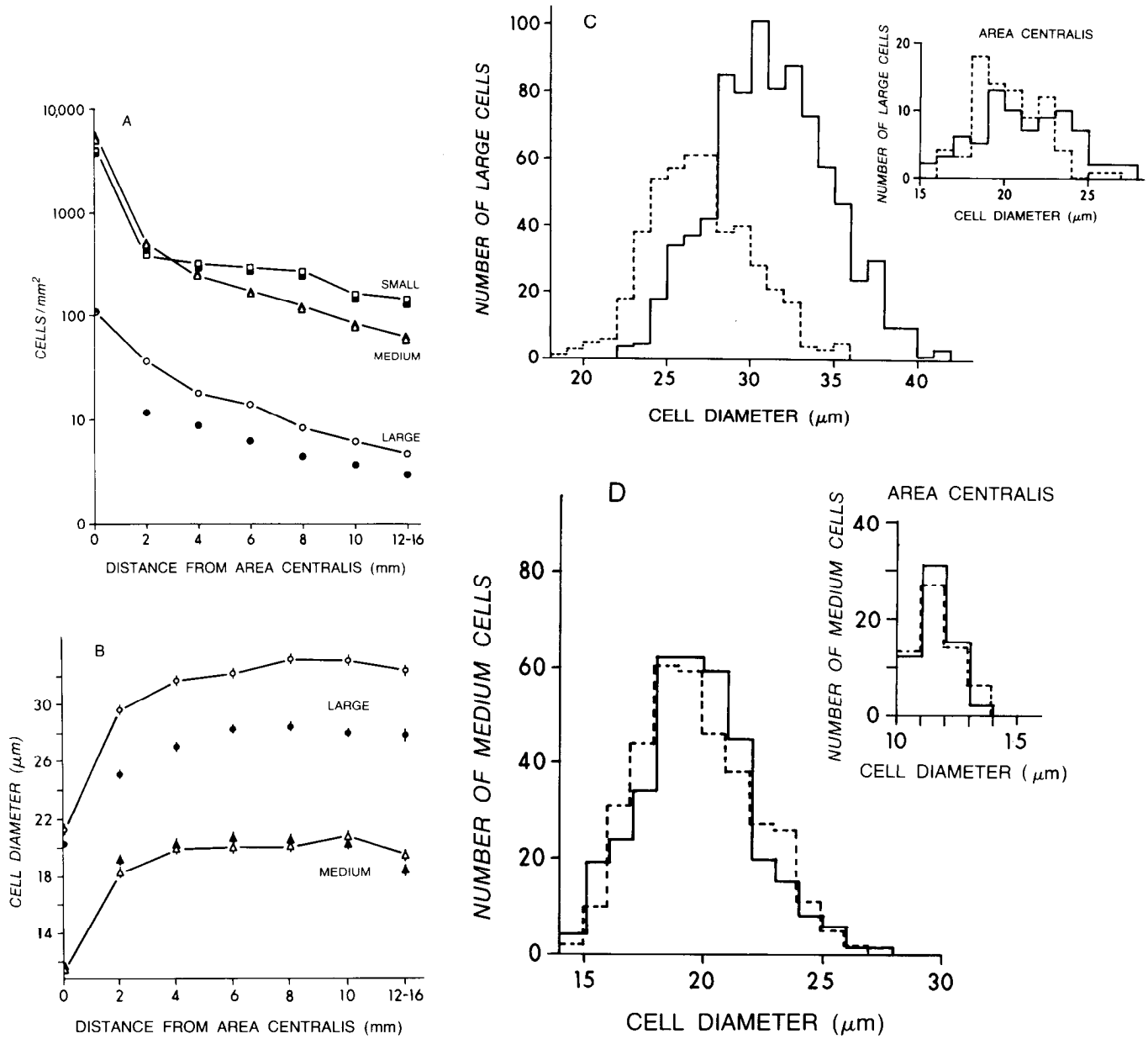

Figure 8. *A*, Ganglion cell counts from a 2,5-HD-dosed cat (*solid symbols*) that survived 8 months after dosing (cat 120), and a control (cat 74) (*open symbols*) from Nissl-stained retinal whole mounts. Cell density (per mm^2) is plotted as a function of distance from area centralis for large (*circles*), medium (*triangles*), and small (*squares*) ganglion cells. At area centralis, each *point* represents one area counted for each cell type. For large cells outside area centralis, each *data point* represents an average of 6 to 11 sampled retinal locations. For medium and small cells outside the area centralis, each *data point* represents an average of 2 to 3 sampled locations. *B*, Cell diameter of large cells (*circles*) and medium cells (*triangles*) as a function of distance from area centralis for the dosed (*filled symbols*) and control (*open symbols*) cats. *Error bars* are ± 1 SEM. *C*, Soma diameter histograms for large ganglion cells from area centralis (*inset*) and 2 to 16 mm eccentricity for the dosed (*dotted lines*) and control (*solid lines*) cats. Seventy-eight cells were included for area centralis in the control cat, and 79 for the dosed cat. Histograms for 2 to 16 mm eccentricity included 831 cells for the control cat and 460 for the dosed cat. *D*, Soma diameter histograms of medium ganglion cells. See above for details. Sixty cells contributed to the histograms of area centralis for each cat, and 360 to the histograms for 2 to 16 mm.

anterograde and retrograde axonal transport are reduced by 2,5-HD (Sahenk and Mendell, 1981), although these effects may be in part secondary to neurofilament accumulation (Griffin et al., 1977). Graham et al. (1982) have emphasized the importance of neurofilaments by postulating that covalent cross-linking of neurofilamentous proteins by 2,5-HD underlies the axonal changes. Neurofilamentous swellings are first seen at the distal nodes of Ranvier, suggesting that constriction at the nodes prevents cross-linked neurofilaments from moving further down the axon. There is a proportionately greater constriction at the node in larger than in smaller fibers (Spencer and Schaumburg, 1975; Cavanagh, 1982), which may account for preferential effects in large fibers. The difference in the nature of transport in the axons of α- and β-cells cannot be determined from the present study. Although the intensity of HRP label was greatly reduced in large cells, some reaction product was found in virtually all α-cells. This suggests only a partial reduction in the rate of uptake or transport, and the possibility that the magnitude of the difference in transport might vary with survival time. Sahenk and Mendell (1981) found reductions in both rate and amount of retrogradely transported material in the sciatic nerve of 2,5-HD exposed animals. However, their results indicate that the magnitude of this effect did not diminish with longer survival times. A similar conclusion can be drawn from

the present failure to find any differences in label after 24- or 48-hr survival times.

A second difference between labeled α- and β-cells in the present study was the appearance of the reaction product. While the label in β-cells showed a granular appearance, that in α-cells had few purple-black granules and consisted instead of a blue-green and rather uniform increase in density. This type of diffuse label has been seen in other studies (Adams and Warr, 1976; Vanegas et al., 1978) and is thought to represent a label that has only recently reached the cell body. A granular label, like that seen in β-cells in the present study, may be organized from the diffuse label if time and label accumulation are sufficient. Thus, the diffuse label in α-cells appears to follow from delayed or reduced transport in these cells.

Long-term effects of 2,5-HD. The ganglion cell counts for the normal cat obtained in the present study are comparable to the values reported by others (e.g., Wassle et al., 1975; Stone, 1978; Hughes, 1981). The only difference is a lower number of large cells encountered in area centralis (120 versus 200/mm^2). This apparent discrepancy may be due to the fact that we sampled a relatively large area (0.67 mm^2), which included lower density portions of the retina (100/mm^2). Normal control values (200 large cells/mm^2) were obtained for both cats 120 and 74 when our counts were restricted to the area centralis. The cell size data for the control cat in the present study are consistent with those reported by others (Boycott and Wassle, 1974; Wassle et al., 1975; Leventhal, 1982), if one takes into account the variation produced by different staining techniques and measuring procedures.

In the cat that survived for 8 months following dosing (cat 120), we found a profound loss of large-diameter cells at all eccentricities beyond area centralis. The loss ranged from 69% at 2 mm to 50% at the far periphery. The overall large cell loss in this cat was approximately 49%. Our data also showed that the remaining α-neurons underwent considerable shrinkage. Since the cells were classified into the three categories on the basis of soma size, it was possible that large cell shrinkage could account for at least a portion of the large cell loss. The reduced size of these shrunken α-cells could have shifted them into the medium cell category. This is particularly likely at 2 mm eccentricity, the region in which we found a small increase in the diameter of medium cells (Fig. 8*B*) and in which the loss of α-cells was the greatest (69%). Such a contribution of large cells to medium cell counts would not be apparent, since the latter population is very large and exceeds the number of large cells by a factor of 10 to 20.

However, examination of the optic tract and the LGN of this animal revealed widespread but subtle gliosis and a disproportionally reduced number of the largest diameter fibers in the ventral portion of the tract, the area which normally contains large diameter axons (Guillery et al., 1982). The loss of large fibers provides strong evidence that at least a portion of the large cells actually degenerated.

We also noticed a slight shrinkage of the most peripheral (12 to 16 mm eccentricity) medium cells. These ganglion cells are almost as large as the centrally located large cells but are of the same size as medium cells of 4 to 10 mm eccentricity. Since the more peripheral ganglion cells have longer axons, it is possible that the length of axon fibers, in addition to size of cell body and axon diameter, are critical in determining toxicity of 2,5-HD in the retinogeniculate pathway.

Optic tract and LGN. Filamentous axonal swellings, which are now established as an effect of 2,5-HD in the visual system (Schaumburg and Spencer, 1978; Cavanagh and Bennetts, 1981), were also seen in the present study. In fact, in a cat that survived for 55 days after the dosing (cat 109), filamentous swellings were accompanied by degenerating axons and myelin, features of the permanent neuronal damage this agent can produce. Although striking selectivity of damage was found in retrograde transport, visual thresholds, and cell loss, such selectivity was not obvious in the appearance of axonal swellings. One should note that selectivity of swellings for fiber diameter is difficult to determine, since the original fiber diameter of the affected neuron cannot be accurately inferred from the size of the swollen axon. Nonetheless, the fact that neurofilament accumulation and thin myelin was seen in a wide range of axonal cross-sections and that the swellings were observed in all regions of the distal optic tract suggest that this effect was most likely not specific to fiber size.

Thus, we found altered transport and neuronal degeneration only in large cells, although axonal swellings in the optic tract were seen in axons of all sizes. Neurons with smaller axon diameters may have been spared because they do not have such a pronounced constriction at nodes of Ranvier; consequently they may better survive neurofilament cross-linking and accumulation (Cavanagh, 1982).

References

Adams, J. C., and W. B. Warr (1976) Origins of axons in the cat's acoustic striae determined by injection of horseradish peroxidase into severed tracts. J. Comp. Neurol. *170:* 107–122.

Blake, R., and A. di Gianfilippo (1980) Spatial vision in cats with selective neural deficits. J. Neurophysiol. *43:* 1197–1205.

Boycott, B. B., and H. Wassle (1974) The morphological types of ganglion cells of the domestic cat's retina. J. Physiol. (Lond.) *240:* 397–419.

Cavanagh, J. B. (1982) The pattern of recovery of axons in the nervous system of rats following 2,5-hexanediol intoxication: A question of rheology? Neuropathol. Appl. Neurobiol. *8:* 19–34.

Cavanagh, J. B., and R. J. Bennetts (1981) On the pattern of changes in the rat nervous system produced by 2,5-hexanediol. Brain *104:* 297–318.

Cleland, B. G., W. R. Levick, and H. Wassle (1975) Physiological identification of a morphological class of cat retinal ganglion cells. J. Physiol. (Lond.) *248:* 151–171.

Cleland, B. G., T. H. Harding, and U. Tulunay-Keesey (1979) Visual resolution and receptive field size: Examination of two kinds of cat retinal ganglion cell. Science *205:* 1015–1017.

Derrington, A. M., and A. F. Fuchs (1979) Spatial and temporal properties of X- and Y-cells in the cat lateral geniculate nucleus. J. Physiol. (Lond.) *293:* 347–364.

Derrington, A. M. and P. Lennie (1983) The influence of temporal frequency and adaptation level on receptive field organization of retinal ganglion cells in the cat. J. Physiol. (Lond.) *333:* 343–366.

Graham, D. G. , D. C. Anthony, K. Boekelheide, N. A. Maschmann, R. G. Richards, J. W. Wolfram, and B. R. Shaw (1982) Studies of the molecular pathogenesis of hexane neuropathy. Toxicol. Appl. Pharmacol. *64:* 415–422.

Griffin, J. W., K. E. Price, and P. S. Spencer (1977) Fast axoplasmic transport through giant axonal swellings in hexacarbon neuropathy. J. Neuropathol. Exp. Neurol. *36:* 603a.

Griffin, J. W., K. E. Fahnestock, D. L. Price, and L. C. Cork (1983) Cytoskeletal disorganization induced by local application of b,b′-iminodiproprionitrile and 2,5-hexanedione. Ann. Neurol. *14:* 55–61.

Griffiths, I. R., P. A. T. Kelly, S. Carmichael, M. McCulloch, and M. Waterstone (1981) The relationship of glucose utilization and morphological change in the visual system in hexacarbon neuropathy. Brain Res. *222:* 447–451.

Guillery, R. W., E. H. Polley, and F. Torrealba (1982) The arrangement of axons according to fiber diameter in the optic tract of the cat. J. Neurosci. *2:* 714–721.

Hartmann, E., B. Lachenmayr, and H. Brettel (1979) The peripheral critical flicker frequency. Vision Res. *19:* 1019–1023.

Hughes, A. (1975) A quantitative analysis of the cat retinal ganglion cell topography. J. Comp. Neurol. *163:* 107–128.

Hughes, A. (1981) Population magnitudes and distribution of the major modal classes of cat retinal ganglion cell as estimated from HRP filling and a systematic survey of the soma diameter spectra for classical neurones. J. Comp. Neurol. *197:* 303–339.

Hylkema, B. S. (1942) Examination of the visual field by determining the fusion frequency. Acta Ophthalmol. *20:* 181–193.

Ikeda, H., and M. J. Sheardown (1982) Aspartate may be an excitatory transmitter mediating visual excitation of "sustained" but not "transient" cells in the cat retina: Iontophoretic studies *in vivo*. Neuroscience *7:* 25–36.

Illing, R. -B., and H. Wassle (1981) The retinal projections to the thalamus in the cat: A quantitative investigation and a comparison with the retinotectal pathway. J. Comp. Neurol. *202:* 265–285.

Jones, H. B., and J. B. Cavanagh (1982) Recovery from 2,5-hexanediol

intoxication of the retinotectal tract of the rat. Acta Neuropathol. (Berl.) *58:* 286–290.

Kornguth, S. E., P. D. Spear, and E. Langer (1982) Reduction in numbers of large ganglion cells in cat retina following intravitreal injection of antibodies. Brain Res. *245:* 35–45.

Lehmkuhle, S., K. E. Kratz, S. C. Mangel, and S. M. Sherman (1980) Spatial and temporal sensitivity of X- and Y-cells in dorsal lateral geniculate nucleus of the cat. J. Neurophysiol. *43:* 520–541.

Lennie, P. (1980a) Parallel visual pathways. Vision Res. 20: 561–594.

Lennie, P. (1980b) Perceptual signs of parallel pathways. Philos. Trans. R. Soc. Lond. (Biol.) *290:* 23–37.

Leventhal, A. G. (1982) Morphology and distribution of retinal ganglion cells projecting to different layers of the dorsal lateral geniculate nucleus in normal and Siamese cats. J. Neurosci. *2:* 1024–1042.

Leventhal, A. G., J. Keens, and I. Tork (1980) The afferent ganglion cells and cortical projections of the retinal recipient zone (RRZ) of the cat's "pulvinar complex." J. Comp. Neurol. *194:* 535–554.

Linsenmeier, R. A., L. J. Frischman, H. G. Jakiela, and C. Enroth-Cugell (1982) Receptive field properties of X- and Y-cells in the cat retina derived from contrast sensitivity measurements. Vision Res. *22:* 1173–1183.

Mendell, J. R., and Z. Sahenk (1980) Interference of neuronal processing and axoplasmic transport by toxic chemicals. In *Experimental and Clinical Neurotoxicology*, P. S. Spencer and H. H. Schaumburg, eds., pp. 139–160, Williams & Wilkins, Baltimore.

Mesulam, M. -M. (1978) A tetramethyl benzidine method for the light microscopic tracing of neural connections with horseradish peroxidase (HRP) neurohistochemistry. Short Course, Society for Neuroscience, St. Louis, MO.

Mesulam, M. -M., and D. L. Rosene (1979) Sensitivity in horseradish peroxidase neurohistochemistry: A comparative and quantitative study of nine methods. J. Histochem. Cytochem. *27:* 763–773.

Morrell, J. I., L. M. Greenberger, and D. W. Pfaff (1981) Comparison of horseradish peroxidase visualization methods: Quantitative results and further technical specifics. J. Histochem. Cytochem. *29:* 903–916.

Pasternak, T., W. H. Merigan, D. G. Flood, and D. Zehl (1983) The role of area centralis in the spatial vision of the cat. Vision Res. *23:* 1409–1416.

Peichl, L., and H. Wassle (1979) Size, scatter and coverage of ganglion cell receptive field centres in the cat retina. J. Physiol. (Lond.) *291:* 117–141.

Rowe, M. H., and B. Dreher (1982) Retinal W-cell projections to the medial interlaminar nucleus in the cat: Implications for ganglion cell classification. J. Comp. Neurol. *204:* 117–133.

Sahenk, Z., and J. R. Mendell (1981) Acrylamide and 2,5-hexanedione neuropathies: Abnormal bidirectional transport rate in distal axons. Brain Res. *219:* 397–405.

Schaumburg, H. H., and P. S. Spencer (1978) Environmental hydrocarbons produce degeneration in cat hypothalamus and optic tract. Science *199:* 199–200.

Schaumburg, H. H., and P. S. Spencer (1979) Clinical and experimental studies of distal axonopathy: A frequent form of brain and nerve damage produced by environmental chemical hazards. Ann. N. Y. Acad. Sci. *329:* 14–29.

So, Y. T., and R. Shapley (1979) Spatial properties of X- and Y-cells in the lateral geniculate nucleus of the cat and conduction velocities of their inputs. Exp. Brain Res. *36:* 533–550.

Spencer, P. S., and H. H. Schaumburg (1975) Experimental neuropathy produced by 2,5-hexanedione: A major metabolite of the neurotoxic industrial solvent methyl *n*-butyl ketone. J. Neurol. Neurosurg. Psychiat. *38:* 771–775.

Stone, J. (1978) The number and distribution of ganglion cells in the cat's retina. J. Comp. Neurol. *180:* 753–772.

Stone, J. (1981) *The Wholemount Handbook: A Guide to the Preparation and Analysis of Retinal Wholemounts*, p. 129, Maitland Publications, Sydney, Australia.

Troy, J. B. (1983) Spatial contrast sensitivities of X- and Y-type neurones in cat's dorsal lateral geniculate nucleus. J. Physiol. (Lond.) *344:* 399–417.

Vanegas, H., H. Hollander, and H. Distel (1978) Early stages of uptake and transport of horseradish peroxidase by cortical structures and its use for the study of local neurons and their processes. J. Comp. Neurol. *177:* 193–212.

Wassle, H., and R. -B. Illing (1980) The retinal projection to the superior colliculus in the cat: A quantitative study with HRP. J. Comp. Neurol. *190:* 333–356.

Wassle, H., W. R. Levick and B. G. Cleland (1975) The distribution of the α-type of ganglion cells in the cat's retina. J. Comp. Neurol. *159:* 419–438.